An Unattended Cloud-Profiling Radar for Use in Climate Research

Kenneth P. Moran,* Brooks E. Martner,* M. J. Post,*
Robert A. Kropfli,* David C. Welsh,* and Kevin B. Widener+

ABSTRACT

A new millimeter-wave cloud radar (MMCR) has been designed to provide detailed, long-term observations of nonprecipitating and weakly precipitating clouds at Cloud and Radiation Testbed (CART) sites of the Department of Energy's Atmospheric Radiation Measurement (ARM) program. Scientific requirements included excellent sensitivity and vertical resolution to detect weak and thin multiple layers of ice and liquid water clouds over the sites and long-term, unattended operations in remote locales. In response to these requirements, the innovative radar design features a vertically pointing, single-polarization, Doppler system operating at 35 GHz (K_a band). It uses a low-peak-power transmitter for long-term reliability and high-gain antenna and pulse-compressed waveforms to maximize sensitivity and resolution. The radar uses the same kind of signal processor as that used in commercial wind profilers. The first MMCR began operations at the CART in northern Oklahoma in late 1996 and has operated continuously there for thousands of hours. It routinely provides remarkably detailed images of the ever-changing cloud structure and kinematics over this densely instrumented site. Examples of the data are presented. The radar measurements will greatly improve quantitative documentation of cloud conditions over the CART sites and will bolster ARM research to understand how clouds impact climate through their effects on radiative transfer. Millimeter-wave radars such as the MMCR also have potential applications in the fields of aviation weather, weather modification, and basic cloud physics research.

1. Introduction

Clouds are immensely important factors in governing climate by means of their effects on the transfer of radiant energy through the atmosphere, in addition to their importance as a vital link in the hydrological cycle. The Committee on Earth Sciences of the U.S. Global Change Research Program (CES 1989) recognized this importance when it identified the need for improved understanding of the role of clouds in climate as its highest priority for climate change research. The CES emphasized that the single largest uncertainty in determining the climate sensitivity to either natural or anthropogenic changes is caused by clouds

through their effects on radiation and their role in the hydrological cycle. Observational information about clouds and their radiative properties was recognized to be sorely lacking.

The Department of Energy responded to the CES recommendation by initiating its long-term, international Atmospheric Radiation Measurement (ARM) program (Stokes and Schwartz 1994) to improve the representation of clouds and their radiative properties in climate models. Since that time, the ARM program has been a stimulus to many climate research activities; the one highlighted here is the development of an unattended millimeter-wave (mm wave) radar for continuous observation of cloud properties that have significant influence on radiative transfer through the cloudy atmosphere. These cloud properties may be classified as macrophysical or bulk, such as layer heights, thicknesses, number of layers, horizontal extent, and microphysical, such as particle sizes, concentrations, and ice and liquid water mass content. They determine the effects that clouds have on upwelling and downwelling radiation. Remote sensing instru-

---

*NOAA/Environmental Technology Laboratory, Boulder, Colorado.
+Pacific Northwest National Laboratory, Richland, Washington.
Corresponding author address: Kenneth P. Moran, NOAA/ETL, 325 Broadway, Boulder, CO 80303.
E-mail: kmoran@etl.noaa.gov
In final form 13 November 1997.

ments such as radars and lidars, in combination with radiometers, are particularly attractive for attaining these observations because they can continuously monitor vertical profiles of important cloud properties. The episodic nature of in situ cloud measurements from research aircraft or balloon sondes, although very useful, cannot match these continuous monitoring capabilities.

Short-wavelength (λ) mm-wave radars are especially well suited for cloud monitoring because of their combination of excellent sensitivity and spatial resolution. The sensitivity advantage results from the inverse fourth-power dependence of echo intensity on wavelength when small-diameter (D) particles are observed ($D \ll \lambda$). Excellent spatial resolution is also readily achieved in range and in beamwidth with short-wavelength radars. These advantages are achieved without the need for extremely powerful transmitters or huge antennas. A number of groups have recently developed millimeter-wave "cloud" radars to observe various cloud macrophysical and microphysical properties from the ground and from aircraft (e.g., Kropfli and Kelly 1996; Clothiaux et al. 1995; Sekelsky and McIntosh 1996). Proposed satellite-borne systems for three-dimensional cloud monitoring on a global scale are the logical, ultimate extension of this technology (Fox and Illingworth 1997).

In this article we describe one of the newest mm-wave cloud radars, an unattended system now in operation at ARM's Southern Great Plains (SGP) Cloud and Radiation Testbed (CART). It is, perhaps, the world's first truly operational, unattended cloud radar for climate research. This radar and others essentially identical to it were designed and are being constructed by the National Oceanic and Atmospheric Administration's Environmental Technology Laboratory (NOAA/ETL) specifically for long-term, unattended operation at ARM CART sites at a few climate-strategic locales worldwide.

2. Context and background

Table 1 compares typical characteristics of three general types of meteorological radars that cover a wide range of operating frequencies; in order of decreasing wavelength, these include wind profilers, storm-surveillance–precipitation radars, and cloud radars. The millimeter wavelengths used by the cloud radars are about an order of magnitude shorter than those used by storm surveillance radars, such as the 10-cm wavelength (S band) WSR-88D (NEXRAD) operated by the National Weather Service. They are about two orders of magnitude shorter than the 74-cm wavelength (UHF) used by the NOAA Wind Profiler Network. All three types of radars can detect clouds to some degree (White et al. 1996).

The large antennas and powerful transmitters used in most precipitation radars, like the WSR-88D, make it possible for them to detect nonprecipitating clouds within a range of several kilometers (e.g., Knight and Miller 1993). However, they are generally unable to fully utilize this capability for a number of reasons, including relatively coarse spatial resolution, ground clutter, and operational mission priorities. WSR-88D cloud observations within about 15 km of the antenna are compromised by ground clutter and by the operational scan sequences, which are limited to low elevation angles. On the other hand, clutter does not constrain mm-wave radar from looking as close as 100–200 m because the signal-to-clutter ratio is 43 dB greater for an 8-mm-wavelength radar than for a

TABLE 1. Characteristics for three types of meteorological radars: *typical* values.

Primary purpose	Wavelengths	Range resolution	Max range coverage	Rain effects
Clear-air wind profiling	6 m–33 cm (VHF) (UHF)	60–500 m	5–20 km	Attenuation not a problem
Precipitation surveillance	10–3 cm (S band)(X band)	150–1000 m	100–450 km	Light-moderate attenuation
Cloud observations	8–3 mm (K_a band)(W band)	30–90 m	10–30 km	Severe attenuation

10-cm-wavelength radar (Kropfli and Kelly 1996). This is true even if the beam patterns for the two radars are identical. In addition, the relatively coarse resolution (250–1000 m) of the WSR-88D and the restrictive scanning procedures of its operational storm-surveillance mission are not well suited for continuous and detailed profiling of clouds. These radars were designed for a different primary task—the observation of precipitation and severe weather—and they perform this mission well. Their ability to detect some clouds while scanning may be a useful extension of these duties (Miller et al. 1997). However, they are not the best choice if the primary objective is observing the quantitative macro- and microphysical details of nearby nonprecipitating clouds.

Even radar wind profilers, operating at much longer wavelengths, possess limited cloud detection capability (White et al. 1996; Orr and Martner 1996) in addition to good precipitation detection capability (Ralph et al. 1995). A new adaptation of wind profiler technology for profiling precipitation at S band also has demonstrated its potential for observing stronger-reflectivity regions of clouds (Ecklund et al. 1995) with moderate temporal and spatial resolution. However, conventional wind profilers are designed primarily to observe advecting atmospheric refractive index gradients in the clear atmosphere. Their long wavelengths are advantageous for this, but, as a consequence, they generally lack the sensitivity to detect small cloud hydrometeors.

Although precipitation and wind-profiling radars provide useful cloud information in some circumstances as an added benefit to their primary functions, it is the mm-wave systems that are specifically designed for finescale, quantitative observations of clouds. These radars exploit the inherent short-wavelength sensitivity advantage for detecting the small cloud particles and the superior resolution associated with their very narrow beams and short pulses. A typical range resolution for the mm-wave systems is about 50 m (Table 1), which is suitable for revealing the intricate structure and motions that are valuable for assessing many basic cloud processes. Beamwidths of 0.2°–0.3° yield lateral resolutions of 35–50 m at a height of 10 km for a vertically directed beam.

The mm-wave radars receiving the most emphasis in atmospheric research today are those operating at frequencies in the atmospheric windows near 35 GHz (λ = 8.7 mm, K_a band) and 94 GHz (λ = 3.1 mm, W band). The primary disadvantages of using radars with such short wavelengths are attenu-

ation by rainfall and limited range coverage, compared to precipitation radars. Attenuation by rain at these wavelengths is severe; this restricts the collection of useful data in or through precipitation to situations involving only very light rain, drizzle, or snowfall. The short attenuating paths associated with a vertically pointing system reduce the impact of this problem somewhat. Attenuation by cloud liquid water and by water vapor, although generally not serious, is greater at the shorter of these two wavelengths, thus favoring the use of K_a band, especially for ground-based systems. Ice crystals and snowfall produce minimal attenuation at these wavelengths; thus, even heavy snowstorms cause no significant attenuation problem for mm-wave radar observations. The W-band radars have an important advantage in smaller and lighter hardware components, which favors their use on airborne and satellite systems.

The use of mm-wave radars to monitor clouds is an updated technology rather than a new discovery. The U.S. Air Force developed 35-GHz radars for use at many air bases in the late 1960s and early 1970s. These AN/TPQ-11 radars were vertically pointing systems and did not have Doppler or dual-polarization capabilities (Paulsen et al. 1970). However, they had good sensitivity and depicted cloud structure overhead fairly well. Unfortunately, they were plagued by recurring hardware maintenance problems including frequent failures of their high-power magnetron transmitters. These problems prompted the air force to decommission the radars in the 1970s. However, there were enough positive results from these fragile instruments to stimulate further developments with mm-wave radar by a few research groups in the 1980s (e.g., Pasqualucci et al. 1983; Hobbs et al. 1985; Lhermitte 1987). Progress intensified in the 1990s in response to an international urgency to better understand the important role that clouds play in climate change. Coincidentally, major radar engineering advances were becoming available at millimeter wavelengths. New or substantially upgraded mm-wave cloud radars were constructed and employed for various cloud studies by several groups (e.g., Albrecht et al. 1990; Kropfli et al. 1990; Pazmany et al. 1994; Clothiaux et al. 1995).

Work at ETL with 35-GHz radars began in the early 1980s with development of its NOAA/K radar. Through a process of continuing upgrades, this radar is still in active service. NOAA/K is a transportable system with a high-power magnetron transmitter; it possesses Doppler, dual-polarization, and scanning

capabilities. In the early 1990s a new high-performance antenna and unique polarization features were added (Kropfli et al. 1990; Kropfli and Kelly 1996). NOAA/K continues to be used extensively for a variety of cloud studies around the world.

Although it can operate unattended for a day or so, NOAA/K is definitely a "research" system that normally requires attention by an engineer and a scientist during operations. Its ability to reveal the finescale structure of most visible nearby clouds, including multiple layer situations (Martner and Kropfli 1993), was the inspiration for ETL to propose the development of a new, unattended cloud radar for ARM. Aside from using the same wavelength (8.7 mm), however, the new radar's innovative design bears little resemblance to that of NOAA/K. ETL is constructing five of the unattended systems, known as millimeter-wave cloud radars (MMCR) for ARM, and another for the National Science Foundation's Surface Heat Budget of the Arctic (SHEBA) project. NOAA and Radian International LLC have entered into a Cooperative Research and Development Agreement (CRADA) to transfer this technology to industry for the production, refinement, and marketing of future units.

3. Radar design

The primary ARM scientific requirements for a cloud radar included the needs for excellent sensitivity to detect weak clouds and for high reliability for long-term, unattended operations. The radars are intended to operate for at least 10 years at the ARM CART sites, to help scientists understand the role of clouds in radiative aspects of climate. In response to these requirements, the ETL design features a vertically pointing, single-polarization, 35-GHz Doppler system that uses a low-peak-power but high-duty-cycle traveling wave tube amplifier (TWTA) transmitter for reliability and a high-gain antenna and pulse-compressed waveforms for heightened sensitivity. The radar design philosophy emphasizes the use of commercial off-the-shelf (COTS) subsystems, including its primary signal processor, which is the same as used in commercially available wind profilers. Use of COTS components makes field maintenance easier to manage.

The first MMCR (Fig. 1) began operations at ARM's CART site in northern Oklahoma in November 1996. The radar transmits only 100 W of peak power, but it uses a high duty cycle of up to 25% to achieve sufficient average power levels for cloud de-

tection. The Oklahoma unit uses a 3-m-diameter antenna with a simple, tilted radome; it has a beamwidth of 0.2° (full width, half power). Subsequent units bound for CART sites in the tropical western Pacific and Alaska will use a 2-m antenna for easier transport. Excluding the antenna, the entire radar hardware weighs about 140 kg and occupies about 2 m^3 of space. It is housed at one end of a climate-controlled sea container, which is approximately 2.5 m $\times$ 2.5 m $\times$ 6.0 m in overall size.

Estimates of reflectivity, mean vertical velocity, and Doppler spectrum width are recorded simultaneously at each gate, typically from 0.1 to 10.0 km or 15.0 km above ground level (AGL). The Doppler processing to determine these first three moments of the spectrum is by fast Fourier transform (FFT) techniques, typically using 64 FFT points and resulting in Doppler velocity resolution of about 10 cm s^{-1}. Coherent and spectral averaging of the data are also employed in the processing. In a special mode, the full Doppler spectrum can also be recorded, although this mode is not routinely used because of greatly expanded data rates. Most of the radar's operating parameters are adjustable at the user's discretion. For example, the sampling dwell time can be varied from less than 1 s to a few minutes, with corresponding ef-
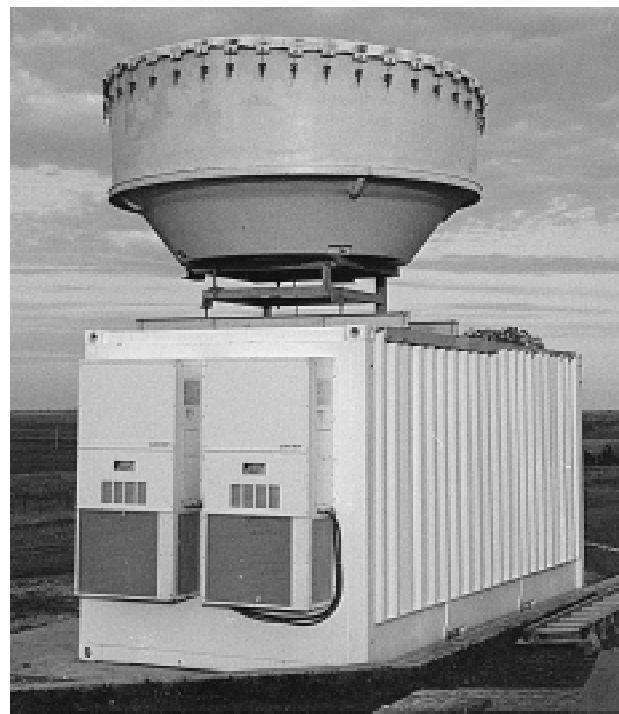

Fig. 1. The MMCR at the SGP CART site in northern Oklahoma.

fects on sensitivity (which is proportional to the square root of dwell time).

The heart of the MMCR is the traveling wave tube amplifier (TWTA), which became commercially available at this wavelength in the early 1990s. These amplifiers typically have much longer lifetimes than magnetrons, but they cannot generate nearly as much peak power. However, they can operate with duty cycles of several tens of percent, well above magnetron duty cycles, which are typically a fraction of 1%. As a result, TWTAs can deliver an equivalent amount of average power but with a factor of 10 longer lifetime. Since average power, among other factors, determines sensitivity, the availability of TWTAs permits one to design a cloud-detection radar that overcomes AN/TPQ-11's reliability problems while achieving superior sensitivity to detect weaker clouds.

The block diagram in Fig. 2 shows the basic elements of the MMCR. A commercial data system for radar wind profilers, developed by the NOAA Aeronomy Laboratory and Radian International, LLC, is used to generate the transmitted waveforms and to receive the signals, both at a nominal intermediate frequency (IF) of 60 MHz. The up–down converter transforms the transmitted frequency from IF to 34.86 GHz, and vice versa for the return signal. Twin circulators are used to protect the low-noise receiving amplifier during pulse transmission and to inject a known level of radio frequency noise to calibrate the radar. This calibration technique automatically and routinely tests the overall radar system except for the antenna, which was carefully evaluated on an antenna test range before installation. A single, large, vertically pointed antenna (2- or 3-m diameter) is used to transmit pulses and receive signals. The antenna is covered by a tilted, flat radome to protect the precisely shaped antenna surface and to encourage rain and condensation to run off.

Two personal computers (PCs) are used in the design; one is primarily for data acquisition and the other for signal processing and communications. The first, using the OS/2 operating system, controls the radar as if it were a wind profiling system. It coordinates radar functions, generates a full Doppler data stream

(spectra or spectral moments vs altitude), and monitors the radar container environment and various critical system parameters, such as power supply status, TWTA current, and voltage standing wave ratio. Remote control of the radar over the Internet can be exercised through this computer. A real-time display on the PC monitor shows vertical profiles of Doppler spectral data and signal-to-noise ratio. The second PC uses the Solaris operating system. It calibrates and archives processed data locally and communicates it and system status information to the outside world, such as feeding the measurements to ARM's external data system. A single monitor/keyboard can be switched manually to function with either computer. When a critical system failure is sensed, such as excessive environmental temperature, the radar is automatically and gracefully shut down in such a way that it can automatically restart when the problem is corrected.

Complementary binary phase coding is the pulse compression technique used to increase the duty cycle, and hence the average power and sensitivity, of the radar while maintaining the desired resolution. Long transmitted pulses (up to 20 μs) are internally phase-coded with much shorter (typically 0.6 or 0.3 μs) segment "chips." The number of chips N is selectable; 32 is typical. Standard techniques (Schmidt et al. 1979) are used to decode the pulses and retain the range resolution associated with the short, phase-coded segments (90 or 45 m) but with the sensitivity associated with the long pulse.

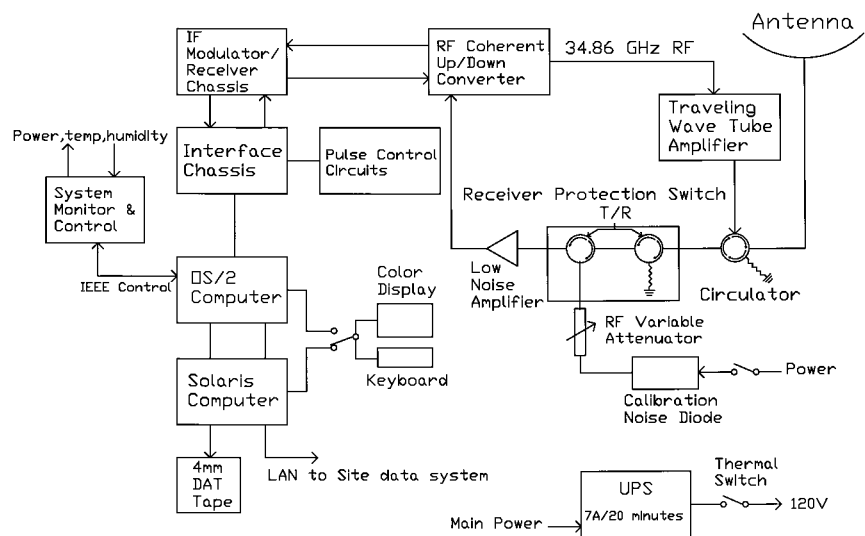Unfortunately, in addition to boosting the system's sensitivity, this and other pulse-compression tech-

FIG. 2. Block diagram of the MMCR.

niques, may generate artifacts known as range sidelobes. These artifacts are most prevalent near regions of clouds that contain stronger vertical Doppler velocities and reflectivities. This results in an apparent "smearing" of echo from intense cloud echoes into the data of the N adjacent height gates. Partial decoding of the signal in the lowest N gates also causes artifacts at those levels. To address these problems, the radar also operates with conventional, noncoded short pulses, which are not subject to range sidelobe effects. These noncoded modes are considerably less sensitive, however, and may fail to detect weaker clouds. By cycling operations between coded and noncoded pulses, the spurious echoes of the coded modes can be identified. An example of the artifacts is discussed in section 4. Work is in progress at ETL and by other groups to develop automated algorithms to recognize and screen these artifacts from the data stream.

Currently, the MMCR routinely cycles sequentially through four data acquisition modes, devoting about 9 s to each. Table 2 shows the modes that were used during the spring of 1997 at the SGP CART in Oklahoma. They include higher and lower resolutions (45 and 90 m), each with coded and noncoded pulse wave forms (32 and 0 bits). Sensitivities, height coverages, Nyquist (folding) velocities, and other features differ between the modes, as shown in the table. Calibration of each mode ensures self-consistent reflectivities among all the modes in the absence of artifacts.

Sequentially cycling through four operating modes also helps the MMCR user to deal with two other data aliasing problems. Any Doppler radar design must contend with a trade-off between the system's Nyquist limit, known as its folding velocity, and its maximum unambiguous range limit, from beyond which distant "second-trip" echoes may contaminate the data at closer ranges. Table 2 shows that the Nyquist and unambiguous range limits for the MMCR's operations in the spring of 1997 varied from 2.8 to 7.5 m s^{-1} and 18.9 to 10.8 km AGL, respectively. When true vertical velocities exceed the Nyquist limit, the MMCR software currently does not unfold these aliased velocities. Furthermore, its reflectivity computations are degraded to some degree, depending on the amount of power received in the folded portions of the spectra. Second-trip echoes are not a very common problem

TABLE 2. ARM MMCR operating characteristics (SGP site—April 1997).

Frequency	34.86 GHz (λ = 8.66 mm, K$_a$ band)
Peak transmitted power	100 W
Max duty cycle	25%
Antenna diameter/on-axis gain	10 ft/57.2 dB
Beamwidth	0.2°

SGP operating mode	1	2	3	4
Interpulse period (μs)	82	126	106	72
Pulse width (ns)	300	600	600	300
Delay (ns)	1200	1200	1200	1200
Gate spacing (ns)	300	600	600	300
Number of coherent avgs	8	6	6	4
Number of spectral avgs	16	21	60	37
FFT length	64	64	64	64
Number of coded bits	32	32	not coded	not coded
Number of gates	220	167	167	220
Duty cycle (%)	11.7	15.2	0.6	0.4
Dwell time (s)	0.7	1.0	2.4	0.7
Sampling interval (s)	9	9	9	9
Min. detectable signal (dBm)	−129	−132	−132	−132
Range resolution (m)	45	90	90	45
Height coverage (km)	0.1–10.0	0.1–15.1	0.1–15.1	0.1–10.0
Unambiguous velocity (m s^{-1})	±3.2	±2.8	±3.4	±7.5
Velocity resolution (m s^{-1})	0.10	0.09	0.11	0.23
Unambiguous range (km)	12.5	18.9	15.9	10.8
Estm. sensitivity (dBZ at 5 km)	−47	−49	−34	−30

for the vertically pointing MMCR because strong cloud targets are infrequently encountered at high altitudes, except perhaps in the Tropics.

The use of the four modes also expands the MMCR's dynamic range of detectable reflectivities and allows it to span the anticipated wide climatological range of cloud conditions more completely. The MMCR's excellent sensitivity is attributable to its short-wavelength, high-average transmitted power, high-gain antenna, moderately long sample times (~1 s), and pulse compression methods. The bottom row of Table 2 lists the sensitivities, estimated by analytical calculations, for each of the four sequential operating modes. The sensitivity of the coded modes (1 and 2) is almost −50 dBZ at a height of 5 km AGL. The corresponding noncoded modes (3 and 4) are about 16 dB less sensitive but have the advantage of being free of range sidelobe artifacts. For comparison, NOAA/K's sensitivity at 5-km height is about −36 dBZ. Recent side-by-side comparisons of the two radars confirm the MMCR's ability, with its coded modes, to detect even weaker clouds than NOAA/K can discern.

4. Examples and applications

The MMCR at the CART in Oklahoma has revealed the intricate structure of a wide variety of clouds. Even with the less sensitive modes that do not use phase coding, the results are impressive. Figure 3 is a 6-h time–height cross section from 12 May 1997 that shows a complicated case of multiple cloud layers including stratus, thin cirrus, and deep altocumulus that produced drizzle and virga. Radar equivalent reflectivity factor, mean vertical Doppler velocity, and Doppler spectrum width are shown in Fig. 3. These moments of the Doppler spectrum were collected with the radar's mode 3, which is not coded and has 90-m resolution (Table 2). The detected reflectivities range from about −45 dBZ in the stratus layer to −35 dBZ in the cirrus and to +13 dBZ in the weakly precipitating regions. The Doppler velocities include the combined effect of particle

fall speeds and vertical air motion; positive values represent downward motion in this image. An abrupt transition to stronger downward motions in the precipitation shaft at about 1.6 km above mean sea level (MSL) and 0900 UTC indicates the effect of accelerating fall speeds as ice particles melt. A small region of folded velocities (> 3.4 m s^{-1} in this mode) appears in the drizzle at this time. Elsewhere, vertical velocities are generally weaker than ±1.5 m s^{-1}. Doppler spectrum width values are very small everywhere except in the drizzle where they reach about 2 m s^{-1}. For vertically pointing measurements such as these, the primary factors that contribute to spectrum width values are turbulent motions at subsample volume
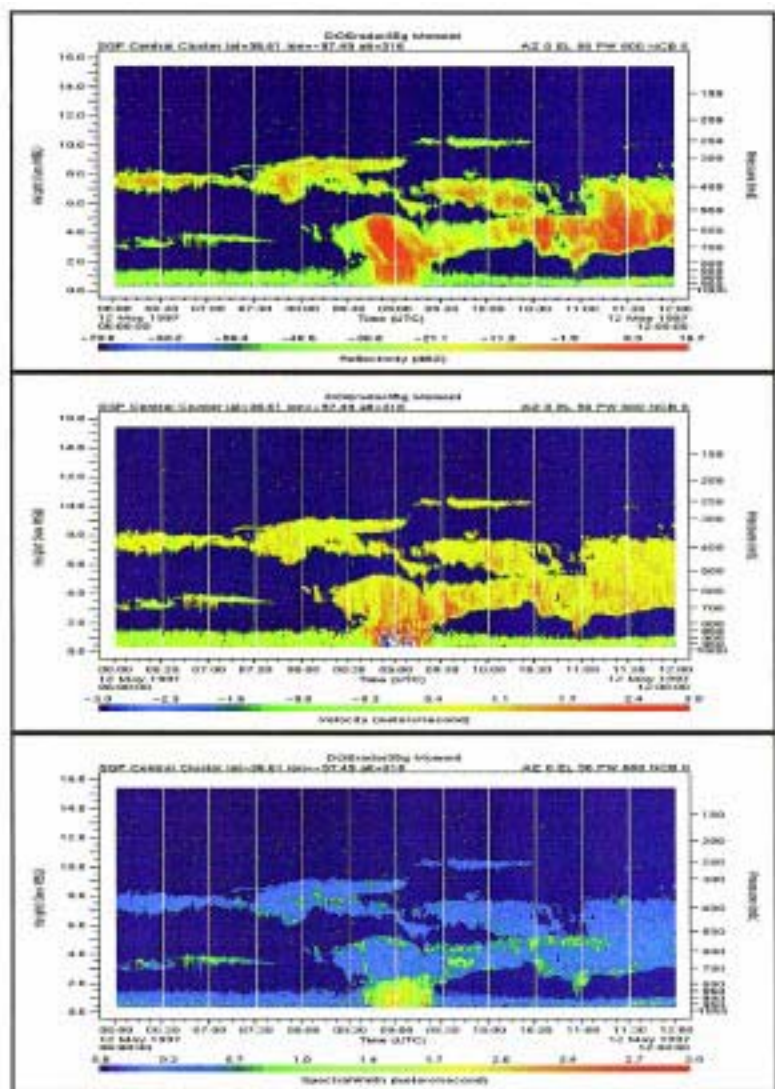

FIG. 3. Time–height cross sections of MMCR data spanning 6 h on 12 May 1997. Parameters shown are radar reflectivity factor (top panel), mean vertical Doppler velocity (middle), and Doppler spectrum width (bottom). Time is labeled in UTC; subtract 5 h for CDT.

scales and the spread of particle fall speeds in the sample. Time–height images of recent MMCR data, similar to these, are routinely made available by ARM and ETL for viewing on the Internet.

Figure 4 is a 23-h time–height image of reflectivity from the MMCR's mode 4 on 10 April 1997. Two to three low to middle cloud layers are visible in this low-sensitivity 45-m resolution mode. Of special interest is the smoothly changing height of a thin midlevel stratiform layer between about 3 and 4 km MSL. The layer descended about 1 km between 0600 and 1200 UTC as a warm front passed the site and then gradually ascended to regain its former altitude as a strong cold front approached. At times, this altostratus exhibited weak convective motions and produced virga that fell into the underlying stratus. Ultimately, the layer merged with thunderstorms that reached the site as the cold front drew near. The entire sequence is roughly similar to classical textbook sketches of cloud conditions on vertical cross sections through cyclonic storms.

Figure 5 is a 9-h time–height reflectivity image from the MMCR's mode 3 on 19 June 1997. It reveals an extensive cirrus overcast, which frequently exhibited weak cellular features and particle fall streaks. The strongest reflectivities were located in these fall streaks, such as the −2 dBZ region at the base of the cirrus echo near 9 km MSL at 2000 UTC where downward motions (not shown) reached 1.4 m s⁻¹, typical of large ice crystal fall speeds. The cloud is obviously far more complex than simple numerical model parameterizations that, by necessity, must depict cirrus as steady, uniform layers. The image also shows a prominent echo layer of about −30 to −20 dBZ below 3 km MSL, which was not caused by cloud. These clear-air boundary layer echoes are very common features in warm seasons at continental locations for cloud and precipitation radars. They are caused by backscattering from millimeter- and smaller-sized insects, seeds, bits of vegetation, and giant dust particles that are suspended by turbulent motions of the convective boundary layer, and which collectively have been described by Lhermitte (1966) as "atmospheric plankton." They are not reflections from clear-air refractive index gradients, which are negligibly weak at mm-wave frequencies.

These boundary layer echoes pose a problem for ARM scientists because they are difficult to distinguish from stratus cloud echoes at the same altitudes. Automated incorporation of cloud-base data from CART lidars or the use of the MMCR's Doppler spectra or spectral width data may help make this distinction. Nonetheless, the MMCR's noncloud boundary layer echo data contain valuable information about boundary layer processes. For example, the diurnal growth and decay of the mixed layer has been approximated from similar data observed with the NOAA/K radar by Martner et al. (1995). In the same manner, the line of enhanced reflectivity in Fig. 5, which slopes upward from 1.0 km MSL at 1500 UTC to 2.3 km at 2000 UTC, represents an average growth rate of 7 cm s⁻¹ for the boundary layer depth on this day. The MMCR's Doppler measurements also provide quantitative information on turbulent motions within the mixed layer, if the targets can be presumed to be predominantly passive tracers of the airflow.

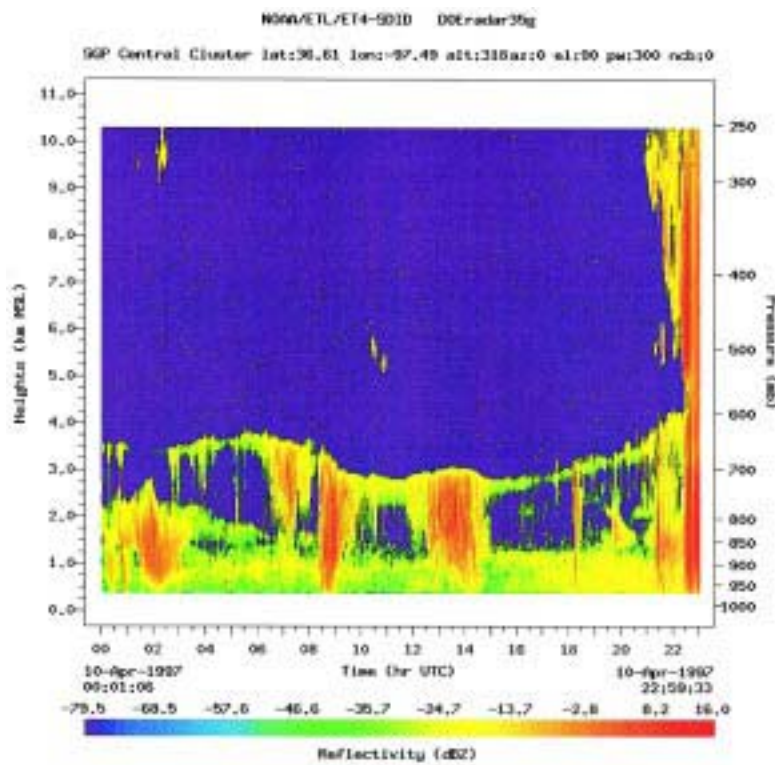As mentioned in section 3, range sidelobe artifacts are an inherent conse-

FIG. 4. Time–height cross section of radar reflectivity factor spanning 23 h on 10 April 1997 from the MMCR's least sensitive mode, which has 45-m resolution and uses no coded bits. A variety of cloud echoes passed over the site as a warm frontal passage was followed by an approaching cold front.

quence of the pulse-compression phase coding used to maximize the MMCR's sensitivity, although they are not always present. Figure 6 shows an example of these spurious echoes. Figure 6a displays a 6-h time–height history of true cloud echoes from mode 4 (noncoded). The corresponding data with the same 45-m resolution from mode 1, which uses 32-bit phase coding, are shown in Fig. 6b. It is apparent that several weaker clouds are revealed by this more sensitive mode. However, there is also a noticeable smearing of echo from the stronger clouds for distances up to 1.44 km above and below the true echoes. Production of these spurious echoes can be analytically predicted based on the cloud echo's Doppler spectrum and the radar's ambiguity function (Wakasugi and Fukao 1985). While ETL is investigating sophisticated techniques for automated identification of the artifacts and removal of their effects using the Doppler spectrum data, simpler threshold techniques are also being tested with the moments data. Figure 6c shows the application of one such recognition technique that uses knowledge of the radar pulse coding and the reflectivity data from mode 4 with a 30-dB threshold to approximate the regions of likely artifacts in mode 1. The darkly shaded regions represent the suspected range sidelobe regions identified by this method.

In addition to providing unprecedented views of cloud structure, quantitative statistical information about cloud-base and cloud-top heights, thicknesses, and numbers of layers can now be generated by mm-wave cloud radars. These radars are able to observe clouds passing overhead and acquire statistical information over long periods of time. Such information cannot be satisfactorily obtained in any other way; research aircraft datasets are too temporally limited for climatological monitoring, and satellite radiometric retrievals of cloud properties, particularly those beneath cloud top, are not yet sufficiently reliable. Statistical cloud information is now becoming available from large datasets obtained with the NOAA/K radar (Uttal and Frisch 1994; Uttal et al. 1995) and other mm-wave radars (Mace et al. 1997). Among other findings, these investigations suggest a prevalence of thin clouds (< 1 km thick) and multiple layers.

Similar analysis of cloud statistics from the MMCR data are now in progress by other ARM scientists. The continuous datasets now issuing from the MMCR will augment earlier preliminary conclusions about cloud statistics based on much shorter radar observational periods, and will allow statistical properties of cloud macrophysical structure to be documented in new climatological regimes and as a function of the meteorological setting, season, and time of day. Although the MMCR is sufficiently sensitive to observe most visible clouds overhead, there are occasions when very diaphanous clouds escape its detection. Furthermore, cloud-base height is often obscured in the radar data when virga is present. Thus, a combination of simultaneous observations by the MMCR and by lidar systems at the CART is the best way to observe virtually all clouds over the site (Uttal et al. 1995).

Exploiting information from remote sensing observations at different wavelengths is a powerful tool for unraveling the microphysical features of clouds that are difficult or impossible to assess with single wavelength observations alone. In combination with other remote sensors, mm-wave radars have proven
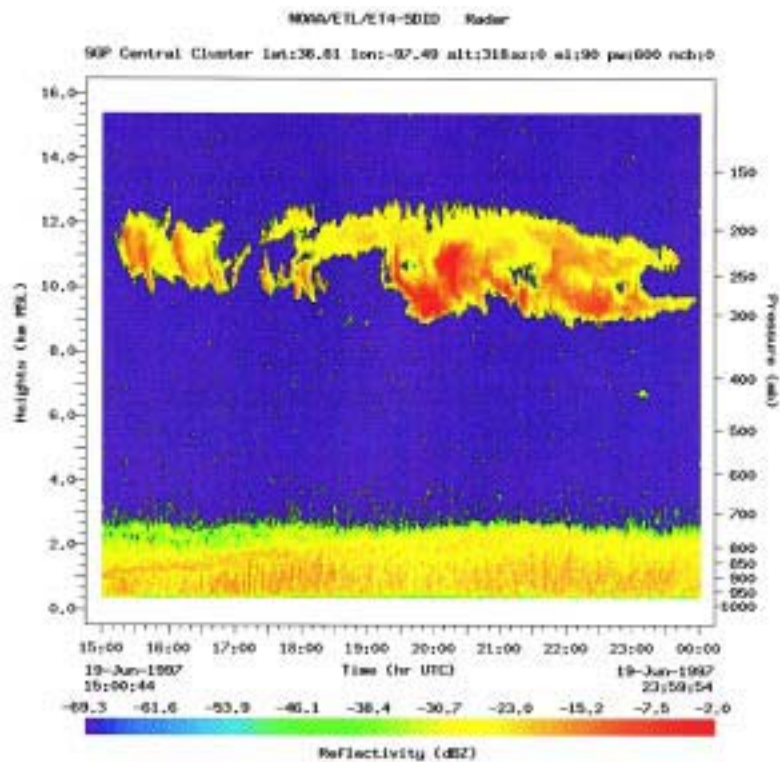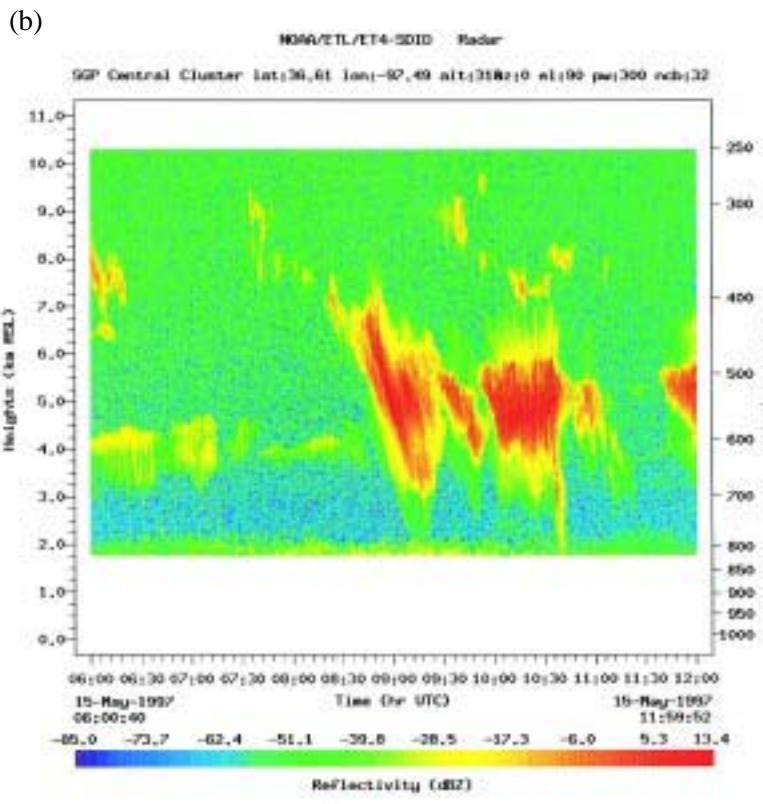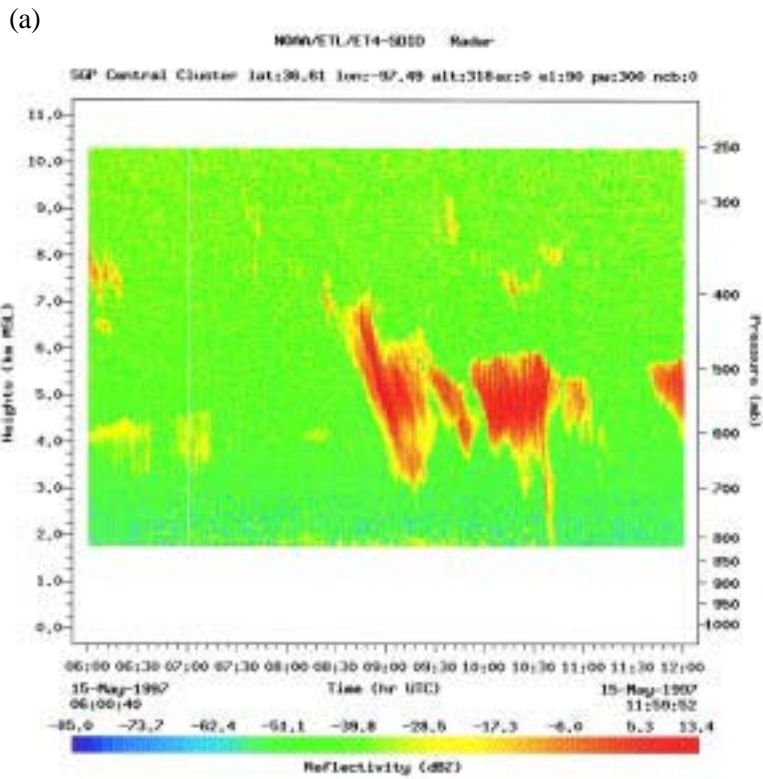

Fig. 5. A 9-h time–height image of radar reflectivity factor on 19 June 1997 showing a persistent cirrus layer above 9 km MSL and a deepening boundary layer echo below 3 km MSL.

(a)

(b)

useful for estimating cloud microphysical parameters such as hydrometeor sizes, concentrations, and ice and liquid water mixing ratios. It will be possible to apply these multisensor methods extensively to the MMCR data at the CART sites because the MMCR operates continuously beside other appropriate active and passive sensors there. For example, MMCR reflectivity data and CART radiometeric measurements of downwelling infrared radiances can take advantage of innovative techniques pioneered by Matrosov et al. (1995) and Matrosov et al. (1997) to estimate vertical profiles or vertically integrated values of median particle size, concentration, and ice mass content in cirrus clouds. A related technique for cirrus clouds uses mm-wave radar and infrared lidar data together to generate vertical profiles of microphysical parameters (Intrieri et al. 1993). Frisch et al. (1995a) developed techniques for deriving profiles of droplet size, concentration, and liquid water content of stratus clouds by combining microwave radiometer and mm-wave radar measurements; similar profiles for drizzle are derived from the radar Doppler data alone. Details of the turbulent structure of clouds can also be revealed by vertically pointing, Doppler, mm-wave radars (Frisch et al. 1995b). These and other single and multisensor methods are expected to be applied appropriately to data from the CART-based MMCRs. It is also expected that the MMCR's Doppler spectra measurements will also eventually be used to estimate the drop size distributions of liquid water clouds explicitly (Gossard et al. 1997).

The MMCR can contribute significantly to the refinement of cloud properties approximated by current and future satellite-borne radiometers.

FIG. 6. Six-hour time–height images of radar reflectivity factor showing an example of range sidelobe artifacts on 15 May 1997. The panels show (a) mode 4 data, which does not use pulse coding and has no artifacts; (b) mode 1 data, which uses 32-bit phase coding to detect weaker clouds but suffers from the artifacts near stronger echoes; and (c, next page) results of a simple algorithm, which uses mode 4 data to determine regions of likely artifacts (dark shading) in the mode 1 data.

Matrosov et al. (1998) present a case study comparison of cirrus particle sizes obtained from aircraft sampling with ground-based radar/radiometer retrievals and a *NOAA-11* satellite radiometer retrieval. Following this example, MMCR-equipped CART sites are prime candidates for operational calibration and validation of satellite cloud parameter retrievals during satellite overpasses such as those in NASA's Clouds and Earth Radiant Energy System (CERES) series, soon to be launched (Weilicki et al. 1996). Although there are difficulties related to the disparate sample volumes of ground-based and space-based instruments, appropriate averaging of the ground-based data should yield useful statistical data to evaluate the cloud products from CERES. The continuous, long-term observations from MMCRs should enable this task to be successfully completed. Once validated, the satellite measurements will extend the monitoring of cloud microphysical properties to a global basis.

In addition to their initial role in climate research, the MMCR and similar mm-wave radars have potential applications in aviation safety, weather modification experiments, and basic research on cloud and precipitation processes. By monitoring the sky at airports in a manner similar to that originally envisioned for the AN/TPQ-11 radars, the modern cloud radars could provide air traffic controllers with information about changing cloud-layer altitudes and intensities that goes far beyond current ceiling and visibility observations. Alone, their data identify cloud-free–precipitation-free altitudes that are also certainly free of icing hazards. In combination with other instruments, such as microwave radiometers, it may be possible to quantitatively evaluate the icing threat at all altitudes in the airport area (Politovich et al. 1995). The relatively small size and power requirements of mm-wave radars, especially at W band, makes airborne applications feasible (Pazmany et al. 1994) and monitoring of in-route aviation cloud hazards possible. Natural cloud process studies and cloud seeding experiments can also benefit from the detailed cloud structure and kinematics measurements that these radars readily provide (Reinking 1995).
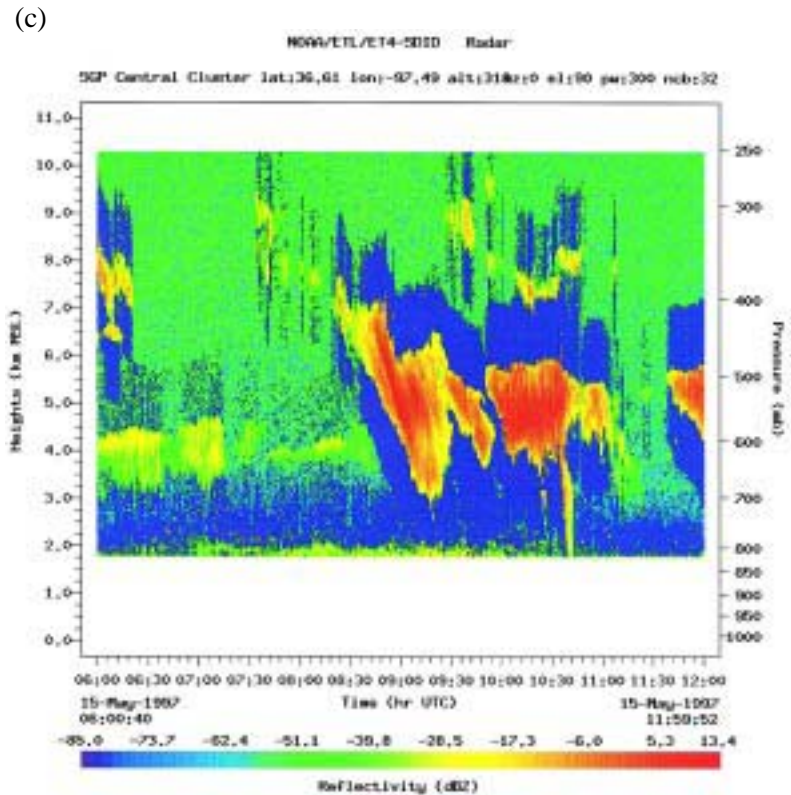
(c)

Fig. 6. *Continued.*

5. Summary

A new mm-wave radar for cloud observations, known as the MMCR, has been described. NOAA/ETL designed these radars for long-term, unattended operations at the Department of Energy's ARM CART sites where they will be used to examine the radiative impacts of clouds on climate. In addition to features for reliable, long-term operation in remote locales, the radar design accommodates requirements for excellent sensitivity and vertical resolution to detect very weak, nonprecipitating clouds, including thin and multiple layers. The MMCR is a vertically pointing, single-polarization, Doppler system operating at 35 GHz. The radar has a 0.2° beamwidth and typically operates with vertical resolutions of 45 and 90 m and height coverage from 0.1 up to 15 km AGL. It uses the same data acquisition processor found in commercially available wind profilers augmented with a second computer for data handling and communications. The MMCR can be operated by remote control, and many of its operating parameters may be adjusted to fit existing conditions or research priorities. The design features a long-life (> 2 yr), low-peak-power TWTA transmitter. Excellent sensitivity and resolution are simulta-

neously achieved in part through the use of high-duty cycles, a high-gain antenna, and phase-coded pulse compression techniques.

The first MMCR was installed at the ARM CART site in Oklahoma in November 1996, and it has operated nearly continuously there (> 97% of the time) for many months with minimal maintenance since then. Additional radars, identical except for slightly smaller antennas, are scheduled to begin operating at CART sites in the tropical western Pacific and in northern Alaska in 1998. The CART site radars are expected to operate for about 10 years at these locations. Another MMCR will be deployed for the SHEBA program on the Beaufort Sea pack ice north of Alaska for one year beginning in late 1997.

The MMCR normally operates with a repetitive sequence of four modes, which collectively optimize sensitivity, height resolution, height coverage, Nyquist limits, and artifact identification. Two modes use phase-coded pulses for the extra sensitivity needed to detect very weak clouds; targets almost as weak as -50 dBZ can be detected at a height of 5 km with these modes. However, the phase-coded data are subject to range sidelobe contamination near stronger cloud targets. The other two modes in the sequence use conventional, short, noncoded pulses that are free of range sidelobe effects, but are less sensitive and may fail to detect weaker clouds.

Early data from the first MMCR have revealed a wide variety of cloud conditions with remarkable, finescale detail. A few illustrative examples are shown in this article. In addition to documenting cloud macrophysical features such as heights and thicknesses, the MMCR data may be combined with simultaneous measurements by CART site radiometers and lidars to estimate microphysical and optical properties of ice and liquid water clouds using recently developed multisensor techniques. Future applications of MMCRs may include their use as ground stations for calibration and evaluation of satellite radiometer retrievals of cloud properties, cloud monitoring for aviation purposes, and basic research on cloud and precipitation processes. Satellite-borne cloud radars for global monitoring of cloud conditions in three dimensions are a logical future extension of the ground-based MMCR's current climate research role.

References

Albrecht, B. A., M. A. Miller, and R. M. Peters, 1990: The development of a surface-based system for observing boundary layer clouds. Preprints, *Ninth Symp. on Turbulence and Diffusion,* Roskilde, Denmark, Amer. Meteor. Soc., 70–73.

Clothiaux, E. E., M. A. Miller, B. A. Albrecht, T. P. Ackerman, J. Verlinde, D. M. Babb, R. M. Peters, and W. J. Syrett, 1995: An evaluation of a 94-GHz radar for remote sensing of cloud properties. *J. Atmos. Oceanic Technol.,* **12,** 201–228.

CES, 1989: *Our Changing Planet, the FY 1990 Research Plan.* U.S. Global Research Program, Office of Science and Technology, 118 pp.

Ecklund, W. L., P. E. Johnston, J. M. Warnock, W. L. Clark, and K. S. Gage, 1995: An S-band profiler for tropical precipitating cloud studies. Preprints, *27th Conf. on Radar Meteorology,* Vail, CO, Amer. Meteor. Soc., 335–336.

Fox, N. I., and A. J. Illingworth, 1997: The potential of spaceborne cloud radar for the detection of stratocumulus clouds. *J. Appl. Meteor.,* **36,** 676–687.

Frisch, A. S., C. W. Fairall, and J. B. Snider, 1995a: Measurement of stratus cloud and drizzle parameters in ASTEX with a K_a-band Doppler radar and a microwave radiometer. *J. Atmos. Sci.,* **52,** 2788–2799.

——, D. H. Lenschow, C. W. Fairall, W. H. Schubert, and J. S. Gibson, 1995b: Doppler radar measurements of turbulence in marine stratiform cloud during ASTEX. *J. Atmos. Sci.,* **52,** 2800–2808.

Gossard, E. E., J. B. Snider, E. E. Clothiaux, B. Martner, J. S. Gibson, R. A. Kropfli, and A. S. Frisch, 1997: The potential of 8-mm radars for remotely sensing cloud drop size distributions. *J. Atmos. Oceanic Technol.,* **14,** 76–87.

Hobbs, P. V., N. T. Funk, R. R. Weiss, and J. D. Locatelli, 1985: Evaluation of a 35-GHz radar for cloud physics research. *J. Atmos. Oceanic Technol.,* **2,** 35–48.

Intrieri, J. M., G. L. Stephens, W. L. Eberhard, and T. Uttal, 1993: A method for determining cirrus cloud particle sizes using lidar and radar backscatter technique. *J. Appl. Meteor.,* **32,** 1074–1082.

Knight, C. A., and L. J. Miller, 1993: First radar echoes from cumulus clouds. *Bull. Amer. Meteor. Soc.,* **74,** 179–188.

Kropfli, R. A., and R. D. Kelly, 1996: Meteorological research applications of mm-wave radar. *Meteor. Atmos. Phys.,* **59,** 105–121.

——, B. W. Bartram, and S. Y. Matrosov, 1990: The upgraded WPL dual-polarization 8-mm-wavelength Doppler radar for microphysical and climate research. Preprints, *Conf. on Cloud Physics,* San Francisco, CA, Amer. Meteor. Soc., 341–345.

Lhermitte, R. M., 1966: Probing air motion by Doppler analysis of radar clear air returns. *J. Atmos. Sci.,* **23,** 575–591.

——, 1987: A 94-GHz Doppler radar for cloud observations. *J. Atmos. Oceanic Technol.,* **4,** 36–48.

Mace, G. G., T. P. Ackerman, E. E. Clothiaux, and B. A. Albrecht, 1997: A study of composite cirrus morphology using data from a 94 GHz radar and correlations with temperature and large-scale vertical motion. *J. Geophys. Res.,* **102,** 13 581–13 593.

Martner, B. E., and R. A. Kropfli, 1993: Observations of multi-layered clouds using K$_a$-band radar. Paper 93-394, *Proc. 31st Aerospace Science Meeting,* Reno, NV, Amer. Institute of Aeronautics and Astronautics, 1–8.

——, A. S. Frisch, and R. M. Banta, 1995: Diurnal evolution of boundary layer turbulence over a boreal forest as observed by Doppler radar. Preprints, *27th Conf. on Radar Meteorology,* Vail, CO, Amer. Meteor. Soc., 485–487.

Matrosov, S. Y., A. J. Heymsfield, J. M. Intrieri, B. W. Orr, and J. B. Snider, 1995: Ground-based remote sensing of cloud particle sizes during the 26 November 1991 FIRE II cirrus case: Comparisons with in situ data. *J. Atmos. Sci.,* **52,** 4128–4142.

——, ——, R. A. Kropfli, B. E. Martner, R. F. Reinking, J. B. Snider, P. Pironen, and E. W. Eloranta, 1998: Comparisons of ice cloud parameters obtained by remote combined sensor retrievals and direct methods. *J. Atmos. Oceanic Technol.,* **15,** 184–196.

Miller, M., J. Verlinde, C. Gilbert, J. Tongue, and G. Lehenbauer, 1997: Cloud detection using the WSR-88D: An initial evaluation. Preprints, *28th Conf. on Radar Meteorology,* Austin, TX, Amer. Meteor. Soc., 442–443.

Orr, B. W., and B. E. Martner, 1996: Detection of weakly precipitating winter clouds by a NOAA 404-MHz wind profiler. *J. Atmos. Oceanic Technol.,* **13,** 570–580.

Pasqualucci, F., B. W. Bartram, R. A. Kropfli, and W. R. Moninger, 1983: A millimeter-wavelength dual-polarization Doppler radar for cloud and precipitation studies. *J. Climate Appl. Meteor.,* **22,** 758–765.

Paulsen, W. H., P. J. Petrocchi, and G. McLean, 1970: Operational utilization of the AN/TPQ-11 cloud detection radar. Air Force Cambridge Labs Instrumentation Papers, Vol. 166, 37 pp.

Pazmany, A. L., R. E. McIntosh, R. Kelly, and G. Vali, 1994: An airborne 95-GHz dual-polarized radar for cloud studies. *IEEE Trans. Geosci. Remote Sens.,* **32,** 731–739.

Politovich, M. K., B. B. Stankov, and B. E. Martner, 1995: Determination of liquid water altitudes using combined remote sensors. *J. Appl. Meteor.,* **34,** 2060–2075.

Ralph, F. M., P. J. Nieman, D. W. van de Kamp, and D. C. Law, 1995: Using spectra moment data from NOAA's 404-MHz radar wind profilers to observe precipitation. *Bull. Amer. Meteor. Soc.,* **76,** 1717–1739.

Reinking, R. F., 1995: An approach to remote sensing and numerical modeling of orographic clouds and precipitation for climatic water resources assessment. *Atmos. Res.,* **35,** 349–367.

Schmidt, G., R. Raster, and P. Czechowsky, 1979: Complementary code and digital filtering for detection of weak VHF radar signals from the mesosphere. *Geosci. Electron.,* **GE-11,** 154–161.

Seklesky, S., and R. McIntosh, 1996: Cloud observations with a polarimetric 33-GHz and 95-GHz radar. *Meteor. Atmos. Phys.,* **59,** 123–140.

Stokes, G. M., and S. E. Schwartz, 1994: The Atmospheric Radiation Measurement (ARM) program: Programmatic background and design of the cloud and radiation test bed. *Bull. Amer. Meteor. Soc.,* **75,** 1201–1221.

Uttal, T., and A. S. Frisch, 1994: Cloud boundaries during ASTEX. Preprints, *Eighth Conf. on Atmospheric Radiation,* Nashville, TN, Amer. Meteor. Soc., 259–261.

——, E. E. Clothiaux, T. P. Ackerman, J. M. Intrieri, and W. L. Eberhard, 1995: Cloud boundary statistics during FIRE II. *J. Atmos. Sci.,* **52,** 4276–4284.

Wakasugi, K., and S. Fukao, 1985: Sidelobe properties of a complementary code used in MST radar observations. *Trans. Geosci. Remote Sens.,* **GE-23,** 57–59.

White, A. B., C. W. Fairall, A. S. Frisch, B. W. Orr, and J. B. Snider, 1996: Recent radar measurements of turbulence and microphysical parameters in marine boundary layer clouds. *Atmos. Res.,* **40,** 177–221.

Wielicki, B. A., B. R. Barkstrom, E. F. Harrison, R. B. Lee, G. L. Smith, and J. E. Cooper, 1996: Clouds and the Earth's Radiant Energy System (CERES). *Bull. Amer. Meteor. Soc.,* **77,** 853–868.